Jernej ČERNELIČ, Gorazd ŠTUMBERGER, Drago DOLINAR

University of Maribor, Faculty of Electrical Engineering and Computer Science

doi:10.15199/48.2015.05.39

Control for Grid Connected Small Wind Turbine System

Abstract *This paper presents a control of a grid connected small wind turbine (SWT) system. The chosen SWT topology consists of a synchronous machine (SM) with excitation winding, a full power back to back converter and an output filter. The control system consists of the hill search type Maximum Power Point Tracking (MPPT) algorithm and the Voltage Oriented Control (VOC). The two control algorithms are interacting over the DC-voltage controller. The proposed control requires small number of measurements that can be reduced to the electrical subsystem of SWT.*

Streszczenie. *W artykule przedstawiono sterowanie małą turbiną wiatrową podłączoną do sieci. System składa się z silnika synchronicznego oraz przekształtnika i filtru wyjściowego. Do sterowania wykorzystano algorytm MPPT i układ VOC.* ***Sterowanie małą turbiną wiatrową podłączona do sieci.***

Key words: small wind turbine, maximum power point tracking (MPPT), voltage oriented control (VOC), wind energy conversion
Słowa kluczowe: mała turbine wiatrowa, algorytm MPPT, przekształtnik

Introduction

Wind energy is becoming a widely used renewable source of energy. The number of wind turbines connected to the electrical grid is increasing rapidly. 35GW of wind power capacity was added in 2013 alone [1]. Most of this power comes from large wind turbine systems which have very high initial cost and can only be built far away from residential areas [2]. However, the demand for small wind turbines (SWT) is increasing too [3-5]. SWTs usually have rated power of 50kW or less and turbine rotor diameter of 15 meters or less according to IEC. The demand for SWTs is increasing because of easier installation and connection to the grid, smaller initial cost and easier placement within the environment.

An array of different topologies of wind turbine (WT) systems can be used for harvesting wind energy. The most widely used topologies include the permanent magnet synchronous machine (PMSG) along with a full power back to back converter or doubly-fed induction generator (DFIG) along with a partial power converter [6-10]. All variable speed wind turbine systems require gearbox or full power back to back converter. The control system usually consists of the WT control and the converter control [7]. The first one controls the output power by changing the pitch angle of the WT blades, whilst the second control system controls the generator side and the grid side converter. The paper proposes a simple control system for low power WTs that does not include the pitch control whilst the converter control is reduced to the grid side converter control (Fig.1).

Description of the small wind turbine system

The discussed system (Fig. 1) consists of a synchronous machine (SM) with excitation winding, diode rectifier, DC-link, three-phase inverter and an output filter. A source of controllable DC voltage is also required to supply the excitation winding of the synchronous machine (SM). SM with excitation winding was chosen because of ability to control output voltage simply by changing excitation voltage. The full power back to back converter was chosen to achieve a variable-speed wind turbine system. It has advantages over gearbox, because power electronic components are lighter, easier to replace and don't require any maintenance. A diode rectifier was selected instead of an active rectifier due to complex control and additional measurements [11]. All laboratory experiments were performed on the existing equipment [12] with the rated power of 10 kVA and rated phase to phase grid voltage of 400V. The full power back to back converter consists of diode rectifier, the DC-link capacitor array with rated voltage of 800V and the IGBT based inverter.

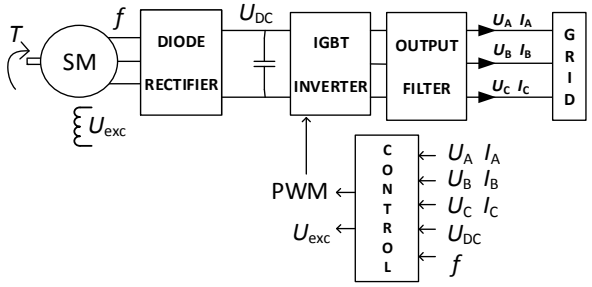

Fig. 1: Schematic presentation of the SWT system

The LCL filter (Fig. 2) is used as an output filter because of very good attenuation ratio, low cost of components, small dimensions and low mass [13]. It consists of an inverter side choke with inductance L_i and resistance R_i, a grid side choke with inductance L_g and resistance R_g, filter capacitors C_f and damping resistors R_d in-between the chokes. The damping resistors R_d are critical for the stability of the system. Their too low resistance values can reduce the damping and increase the total harmonic distortion (THD) which can cause the system instability. However, too high resistance values can cause the unwanted power losses. Any other filter topology can be used but the attenuation ratio must be high enough to meet IEC requirements for connection to the grid regarding THD.

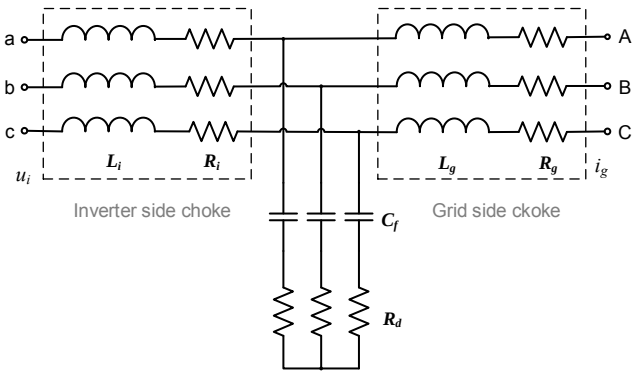

Fig. 2: Schematic diagram of the LCL filter

The parameters of the LCL filter were determined by using a simplified method [14]. This method uses allowed current ripple and switching frequency information for determining the parameters of the filter.

Control OF the Small wind trubine (SWT)

The main idea of proposed control is to increase the excitation voltage of SM in order to increase the three-phase output voltage of SM, which will increase the rectified DC-link voltage. The control of the inverter includes the DC-link voltage controller which prevents the DC-link voltage from rising by transmitting active power *P* to the grid. The power flow from the inverter to the grid depends on the phasors of the inverter and the grid voltages according to (1). By changing the amplitude of inverter voltage *E* it is possible to control the reactive power and by changing the angle *φ* between the inverter voltage *E* and the grid voltage *U* it is possible to control the active power.

$$P = \frac{EU\sin\varphi}{X}$$
$$Q = \frac{EU\cos\varphi - U^2}{X} \quad (1)$$

where: E – RMS value of inverter voltage phasor, U – RMS value of grid voltage phasor, φ - angle between *U* and *E*, X - LCL filter reactance.

The control of the SWT system consists of two parts. The first part controls the output power of the SM by changing excitation voltage based on the output power and speed of the turbine using the Maximum Power Point Tracking (MPPT) algorithm, similar as in [15-16]. The MPPT algorithm (Fig. 3) extracts maximum power from the wind turbine at every given wind speed. Maximum Power Point (MPP) is reached when the output power *P* does not change with the change of turbine speed Ω_m. If the output power is increasing with turbine speed the system has not yet reached the MPP. If the output power is decreasing with increasing turbine speed the system has passed the MPP. This approach can be used due to the wind turbine characteristics (Fig.3), where the MPP changes with the wind speed (v_1<v_2<v_3) whilst the MPPT algorithm must constantly control the output power [17-19]. The MPPT algorithm is the hill climb searching (HCS) type and is based on all 4 possible changes of the output power *P* and the speed of the turbine Ω_m. The changes are described in Table 1. One additional condition that controls the maximum speed of wind turbine must be considered. If the rated speed is already reached, the excitation voltage must increase even more to prevent further acceleration of the turbine. When the critical speed or power is reached the system should shut down and the emergency brake must engage. The speed Ω_m can be obtained through the measured frequency of SM output voltage or it can be calculated directly from one measured SM output voltage using the Phase Locked Loop (PLL) algorithm or similar. The output of MPPT algorithm is the change of excitation voltage by +/- 0.5% of rated excitation voltage U_{exc}. The excitation voltage changes every 1 ms. Frequency of excitation voltage change can be decreased in systems with larger inertia and must be increased in systems with smaller inertia. The increase of excitation voltage U_{exc} increases the output voltage of the synchronous generator which can increase the DC-link voltage U_{DC}.

The second part of the SWT control system controls inverter currents in the synchronous rotating reference frame *dq* using the Voltage Oriented Control with PI controllers (VOC-PI) (Fig. 4) [20-22]. The name comes from the fact that the reference frame is aligned with the grid voltage vector. The measured grid voltages and currents are transformed to the rotating *dq* reference frame using *dq0* transformation. Its angle is determined using the Phase Locked Loop (PLL) algorithm. An error in the PLL algorithm can cause loss of synchronisation that can cause system breakdown.

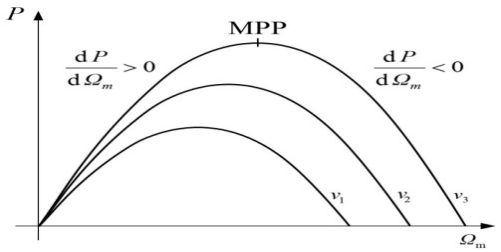

Fig. 3: Maximum Power Point Tracking

Table 1: MPPT algorithm

Change of output power and mechanical speed	Change of excitation voltage
$\frac{dP}{dt} > 0, \quad \frac{d\Omega_m}{dt} > 0$	$\frac{dU_{exc}}{dt} > 0$
$\frac{dP}{dt} < 0, \quad \frac{d\Omega_m}{dt} > 0$	$\frac{dU_{exc}}{dt} > 0$
$\frac{dP}{dt} > 0, \quad \frac{d\Omega_m}{dt} < 0$	$\frac{dU_{exc}}{dt} < 0$
$\frac{dP}{dt} < 0, \quad \frac{d\Omega_m}{dt} < 0$	$\frac{dU_{exc}}{dt} < 0$

A decoupled current controller with voltage feed forward is used in the Voltage oriented control. According to (2) the *d*-axis current controls the active power *p* and the *q*-axis current controls reactive power *q*. Simplified equations (2) are valid only for the grid voltage vector perfectly aligned with the *d*-axis of the *dq* reference frame, where the *q*-axis voltage equals zero (u_q = 0).

$$p = u_d\, i_d$$
$$q = u_d\, i_q \quad (2)$$

where: u_d – d-axis voltage, i_d – d-axis current, i_q – q-axis current

According to Fig. 4, the reference for the *d*-axis current is obtained from DC-link voltage control. Proper gains for this controller were determined experimentally. If the DC link voltage increases for 5V the *d*-axis current must increase for 1A. This sets the proportional gain K_p=1/5 A/V. The required response was achieved by selecting the time constant T_i = 0.02 s. The output of this controller must be subtracted from the value of the *d*-axis current reference. Gains for VOC current controllers were determined using the Ziegler-Nichols method of step response, because of the complexity of the LCL filter transfer function $G_f(s)$. The control-loop contains transfer function of the PI controller, the transfer function of the inverter, which is considered as a first order system, and the transfer function of LCL filter $G_f(s)$ (3) [23].

$$G_f(s) = \frac{I_g(s)}{U_i(s)} = \frac{R_d C_f s + 1}{L_i L_g C_f s^3 + R_d C_f (L_i + L_g) s^2 + (L_i + L_g) s} \quad (3)$$

Where: L_i – inverter choke inductance, L_g – grid choke inductance, C_f – filter capacitor, R_d – damping resistor

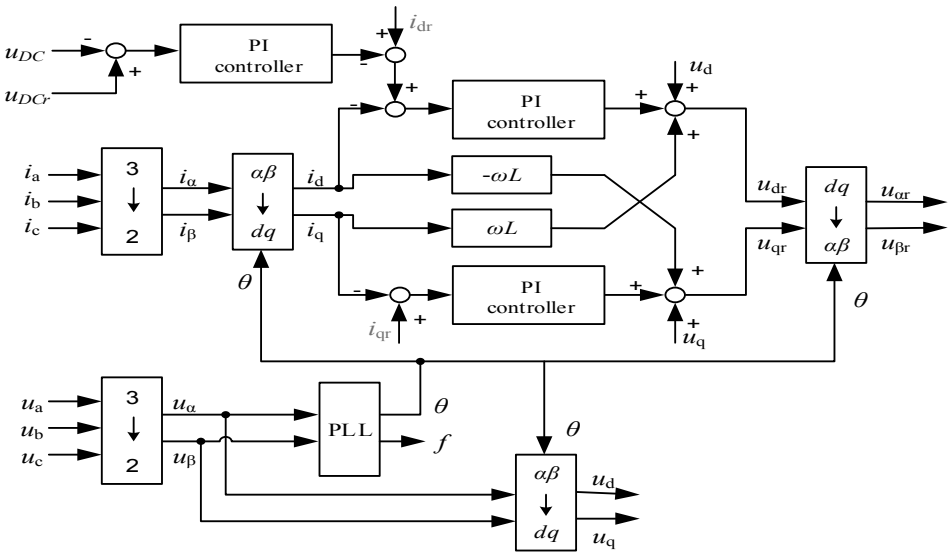

Fig. 4: Voltage Oriented Control with PI controllers (VOC-PI)

The transfer function (3) describes the relationship between the current I_g that flows to the grid and the voltage on the inverter side of the filter. Any other method such as the root locus placement method can be used to determine gains for VOC. Finally the reference voltages u_{dr} and u_{qr} are transformed back to the *αβ* reference frame, where they are used in the space-vector pulse-width modulation (SVPWM).

Normaly, protection functions are implemented in the control algorithm. This system requires protection against the DC-link overvoltage. In the case of overvoltage the synchronous machine must be disconnected first and the inverter must stop working or the SWT system must disconnect from the grid.

Simulation results

In order to evaluate the proposed control, a simulation model was built in Matlab/Simulink using SimPowerSystem library. The synchronous machine torque was changed several times according to Fig. 5 to check how well the controller can follow changes in the wind speed and consequently torque and power on the SM shaft. The initial speed of the wind turbine was set at lower value than the rated speed to check whether the controller can maintain reference speed. A step change in the *q*-axis current reference was also added at 0.7s to show the possibility to generate reactive power. The main system parameters are listed in Table 2.

Table 2: Main system parameters

Rated power = 10kVA	Generator inductance = 9mH
Grid frequency = 50Hz	SM inertia = 25kgm^2
Switching freq. = 10kHz	DC-link voltage = 700V
Grid voltage= 400V	Pole pairs = 8

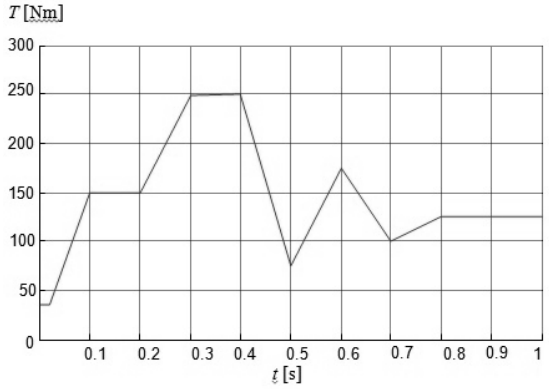

Fig. 5: Changes of synchronous machine torque

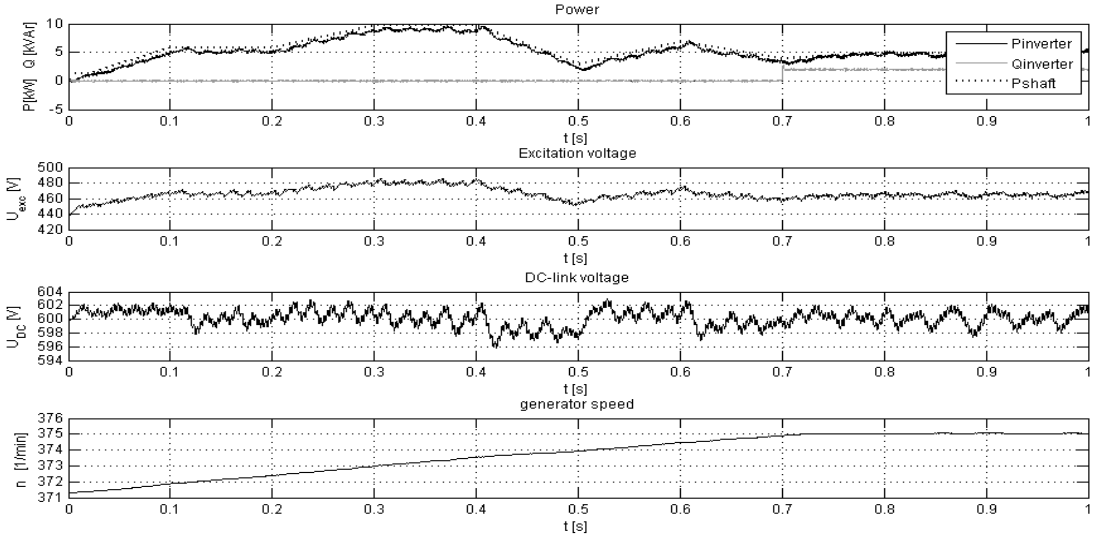

Fig. 6: Simulation results

The simulation results (Fig. 6) confirm the proposed control. The output active power follows the input power on the shaft with very small delay even at rapid changes of torque on the shaft. The output power is lower than the input power because of the acceleration of the wind turbine. The controller is able to stop acceleration at the reference speed of 375 min^{-1}. The DC-link voltage changes are very small and the system is able to generate reactive power along with active power. The DC-link voltage must be higher than the rectified voltage of the grid, because of reactive power generation. This is the reason for the DC-link voltage of 600V. The excitation voltage has the same shape as the active power, because the active power generation is controlled by the excitation voltage of synchronous machine.

Experimental verification

In order to confirm the simulation results the experimental system (Fig.7) was built using a synchronous machine and a DC motor which represented a wind turbine. A back to back converter with an LCL output filter from recent experiment [12] was used to connect the system to the grid. The experimental system was controlled with the proposed control algorithm using the dSpace controller board DS1103. The grid voltages were measured using differential probes whilst the grid currents were measured using LEM current transducers.

The excitation voltage was changed from 58 V to 53 V to show change in the output power (Fig. 9) which dropped from around 3 kW to around 2 kW. The system response was slow because the excitation current dropped slowly due to high inductance of synchronous machine excitation winding. The grid-side phase to phase voltage was reduced to around 300V with transformer to avoid possible overvoltage on the DC-link. In the case of sudden loss of synchronization with the grid and disconnection from the grid during active power generation, the output voltage of synchronous machine could rise due to sudden loss of load. This has to be considered when designing the DC-link and DC-link overvoltage protection. Before the system is disconnected from the grid, the synchronous machine must be disconnected from the DC-link or DC-link rated voltage must be high enough to withstand the voltage rise in the case of sudden loss of load.

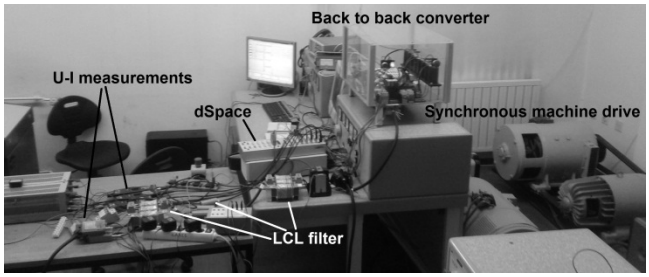

Fig. 7: Experimental system

Some higher-order harmonics can be seen in the grid voltages (Fig. 8) which are the reason for the distorted grid currents. This higher order harmonics can cause oscillations in the *dq* reference frame (Fig. 9) which are particularly high in the cases of high currents and consequently powers. It can be seen that the *dq* reference frame is perfectly aligned with the grid voltage vector, because all voltage appears in the *d*-axis. This applies only at stable voltage and frequency conditions of the grid. The current and power charts have the same shape because the entire voltage vector appears in the d-axis and equations (2) can be applied.

Conclusion

The proposed small wind turbine control system design allows maximum possible active power generation from the torque supplied to the synchronous machine shaft. The experimental verification confirms that the proposed control design enables the control of active power generation simply by changing the excitation voltage of the synchronous machine. The advantage of this control is that the parameters of the wind turbine and the synchronous machine do not have to be exactly known. It performs very well even without measured wind speed or any other parameter of the mechanical subsystem. All necessary measurements are limited to the electrical subsystem. The limited number of measurements reduces the costs of the system. The use of power electronics instead of the gearbox and selection of the synchronous machine with excitation winding further reduce the costs. Independent reactive power generation control is inherited in the proposed system due to the decoupled current controllers in *dq*-axes.

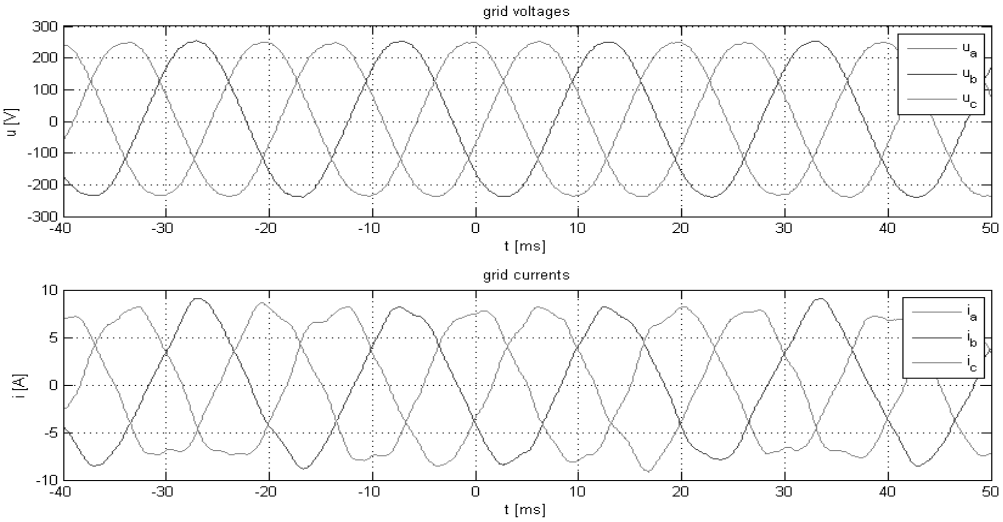

Fig. 8: Grid voltages and currents

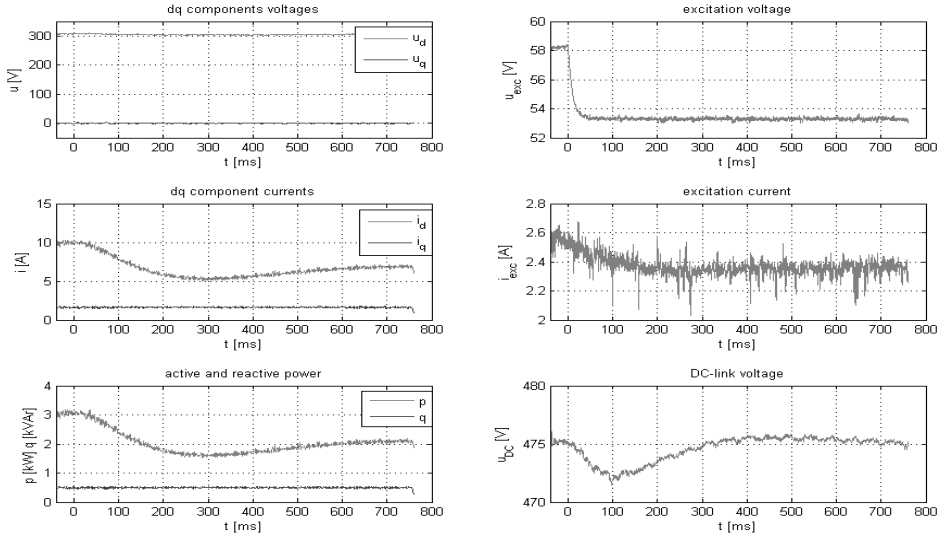

Fig. 9: Experimental results

REFERENCES

[1] Renewables Global Status Report available at http://www.ren21.net/gsr

[2] Vries E., Close up – Vestas V164-8.0 naccele and hub, available at http://www.windpowermonthly.com/article/1211056/

[3] Small Wind World Report 2014 available at http://small-wind.org

[4] Chen Z., Blaabjerg F., Wind turbines – a Cost Effective Power Source, Przeglad Elektrotechniczny (Electrotechnical Review in Polish), No. 5 (2004), 464-469.

[5] Ani, S.O., Polinder H, Ferreira J.A.,Energy, Comparison of Energy Yield of Small Wind Turbines in Low Wind Speed Areas, IEEE Transactions on Sustainable Energy, 4 (2012), no. 1, 42-49

[6] Blaabjerg F., Ma K., Yang Y., Power Electronics – The Key Technology for Renewable Energy Systems, Ecological Vehicles and Renewable Energies proceeding of international conference in Monte Carlo, Monaco, 2014, IEEE, 1-11

[7] Iov F., Blaabjerg F., Power Electronics and Control for Wind Power Systems, in Power Electronics and Machines in Wind Applications proceedings of international conference in Lincoln, USA, 2009, IEEE, 1-16

[8] Chen Z., Guerrero J.M., Blaabjerg F., A Review of the State of the Art of Power Electronics for Wind Turbines, IEEE Transactions on Power Electronics, 24 (2009), No. 8, 1859-1875

[9] Blaabjerg F., Liserre M., Ma K., Power Electronics for Wind Turbine systems, IEEE transactions on Industry Applications, 48 (2011), No. 2, 708-719

[10] Thiringer T., Petersson A., Grid Integration of Wind Turbines, Przeglad Elektrotechniczny (Electrotechnical Review in Polish), No. 5 (2004), 470-475

[11] Buchert K, Fuchs F.W., Comparison of Three Phase Rectifier Topologies in Small Wind Turbines. European Conference on Power Electronics and Applications in Lappeenranta, 2014, IEEE, 1-10

[12] Cernelic J., Stumberger G., Laboratory Realization of Static VAr Compensator, in Compatibility and Power Electronics (CPE) proceedings of the international conference in Ljubljana, Slovenia, 2013, IEEE, 120-125

[13] Liserre, M., Blabjerg, F., Hansen S, Design and Control of an LCL-Filter-Based Three-Phase Active Rectifier, IEEE Transactions on Industry Applications, 41(2005), No. 5, pp 1281-1291

[14] Sun W., Chen Z., Wu X., Intelligent Optimize Design of LCL Filter for Three-phase Voltage Source PWM Rectifier, Power Electronics and Motion Control Conference proceedings of international conference in Wuhan, China, 2009, IEEE, pp. 970-974

[15] Aubree R., Auger F., Dai P., A New Low Cost Sensorless MPPT Algorithm for Small Wind Turbines, Renewable Energies and Vehicular Technology proceedings of international conference in Hammamet, 2012, IEEE, 305-311

[16] Koutroulis E., Kalaitzakis K., Design of a Maximum Power Tracking System for Wind-Energy-Conversion Applications, IEEE Transactions on Industrial Electronics, 53 (2006), No. 2, 486-494

[17] Kazmi S., Goto H., Guo H., Ichinokura O., Review and Critical Analysis of the Research Papers Published Till Date on Maximum Power Point Tracking in Wind Energy Conversion System, in Energy Conversion Congress and Exposition (ECCE) in Atlanta, USA, 2010, 4075-4082

[18] Ling Y., Guoxiang W., Cai X., Comparison of Wind Turbine Efficiency in Maximum Power Extraction of Wind Turbines with Doubly Fed Induction Generator, Przeglad Elektrotechniczny (Electrotechnical Review in Polish), No. 5b (2012), 157

[19] Urtasun A., Sanchis P., Marroyo L., Small Wind Turbine Sensorless MPPT: Robustness Analysis and Lossless Approach, IEEE Transactions on Industry Applications, 50 (2014), No. 6, 4113-4121

[20] Blaabjerg F., Teodorescu R., Liserre M., Timbus A.V., Overview of Control and Grid Synchronization for Distributed Power Generation Systems, IEEE Transactions on Industrial Electronics, 53 (2006), No. 5, 1398-1409

[21] Timbus A., Liserre M., Teodorescu R., Rodriguez P., Blaabjerg F., Evaluation of Current Controllers for Distributed Power Generation Systems, IEEE Transactions on Power Electronics, 24 (2009), No. 3, 654-664

[22] Sedlak M., Stynski S., Kazmierkowski M., Malinowski M., Three-level four-leg flying capacitor converter for renewable energy sources, Przeglad Elektrotechniczny (Electrotechnical Review in Polish), No. 12a (2012), 6

[23] Ahmed K. H., Finney S. J., Williams B. W., Passive Filter Design for Three-Phase Inverter Interfacing in Distributed Generation, Compatibility in Power Electronics proceedings of international conference in Gdansk, Poland, 2007, IEEE, 1-9

[24]

Authors: *Jernej Černelič, University of Maribor, Faculty of Electrical Engineering and Computer Science, Smetanova ulica 17, 2000 Maribor, Slovenia, e-mail: jernej.cernelic@um.si,*
prof. dr. Gorazd Štumberger, University of Maribor, Faculty of Electrical Engineering and Computer Science, Smetanova ulica 17, 2000 Maribor, Slovenia, e-mail: gorazd.stumberger@um.si,
prof. dr. Drago Dolinar, University of Maribor, Faculty of Electrical Engineering and Computer Science, Smetanova ulica 17, 2000 Maribor, Slovenia, e-mail: drago.dolinar@um.si.